RESEARCH ARTICLE

Editorial Process: Submission:08/26/2024 Acceptance:12/17/2024

Proteomic Analysis of Anticancer Effect of *Myo-inositol* in Human Prostate Cancer (DU-145) Cell Line

Mohammad Jahidul Islam[1]*, Sidratul Muntaha[2], Md Mohiuddin Masum[3], Sazia Nowshin[4], Sabia Salam[5], Mominul Haque[6], Myo Wint Zaw[7], Shahriar Jahan[8]

Abstract

Objective: This study investigated the potential anticancer properties of Myo-inositol on the DU-145 prostate cancer cell line. Methods: The DU-145 cells have been treated to different doses of Myo-inositol in order to ascertain the half-maximal inhibitory concentration (IC_{50}) using the trypan blue exclusion assay. The impact of Myo-inositol on proteomic profiles was evaluated using 2D gel electrophoresis and liquid chromatography-mass spectrometry (LC-MS). **Results:** Myo-inositol significantly reduced DU-145 cell viability with an IC_{50} of 0.06 mg/ml ($p<0.05$). Proteomic analysis highlighted marked differences in protein expression between treated and untreated cells, particularly in proteins related to cytoskeletal regulation, apoptosis, and stress response. LC-MS further identified significant alterations in protein profiles, with suppression of proteins like Annexin A2 and Cofilin-1-A in controls, and upregulation of proteins such as Rho GTPase-activating protein, Apoptotic protease-activating factor 1 (APAF1), and TNF receptor-associated factor 2 (TRAF2) in treated samples ($p<0.001$), indicating modulation of key signaling pathways involved in tumor suppression and oncogenesis. **Conclusion:** Myo-inositol exhibits anticancer properties in prostate cancer cells by impacting cell viability and altering protein expression. While promising as an adjunctive treatment, further studies are needed to understand its mechanisms and potential in combination therapies for managing CRPC.

Keywords: Proteomic analysis- Myo-inositol- Human prostate cancer (DU-145) cell line

Asian Pac J Cancer Prev, **25 (12)**, 4447-4455

Introduction

Prostate cancer severely impacts older men, especially those 65 and older [1]. Globally, it is the second most common male condition and the sixth leading cause of cancer fatalities. This cancer is more common in North America, Europe, and Australia due to a complex interplay of hereditary, lifestyle, and environmental factors. Approximately one in eight US men may have this illness. Adjusted for age, male fatalities are 7.7 per 100,000. Despite improved detection and treatment, prostate cancer causes around 1.4 million new cases and 375,000 deaths annually [2]. Treatment options include androgen deprivation therapy (ADT), chemotherapy, and radiation. Due to its hormone therapy resistance, castration-resistant prostate cancer (CRPC) often has poor results. Understanding prostate cancer biology is essential for finding new therapeutic targets and improving methods. This research focuses on androgen receptor signaling abnormalities that cause cancer [3]. Traditional prostate cancer therapies cause fatigue, cardiovascular difficulties, and metabolic disruptions, highlighting the need for better-tolerated alternatives [4]. Natural products and small compounds that regulate critical signaling pathways could improve prostate cancer treatment and outcomes by being safer and more effective [5].

Myo-inositol, the most active of its nine stereoisomers, is essential to cell signaling and metabolism [6]. It forms cell membrane inositol phospholipids and affects insulin signaling, lipid metabolism, and intracellular calcium ion concentration. This precursor of inositol triphosphate (IP_3) plays a crucial role in cell proliferation, death, and differentiation [7]. Myo-inositol and its derivatives limit cell growth and trigger apoptosis in breast, colon, and prostate cancer cell lines via disturbed pathways like the PI3K/Akt pathway. Myo-inositol supplementation may also lower lung cancer risk in high-risk patients, suggesting its promise in cancer prevention and therapy

*[1]Department of Pharmacology. Bangabandhu Sheikh Mujib Medical University, Dhaka, Bangladesh. [2]Department of Biochemistry, Bangabandhu Sheikh Mujib Medical University, Dhaka, Bangladesh. [3]Department of Anatomy, Bangabandhu Sheikh Mujib Medical University, Dhaka, Bangladesh. [4]Department of Surveillance & Immunization, World health organization (WHO), Dhaka. Bangladesh. [5]National Institute of Ophthalmology & Hospital, Dhaka, Bangladesh. [6]Department of Anatomy, Popular Medical College, Dhaka, Bangladesh. [7]Department of Biochemistry, University of Cyberjaya, Malaysia. [8]Department of Molecular Biology, EW Villa Medica, Dhaka, Bangladesh. *For Correspondence: jahidul_islam@bsmmu.edu.bd*

[8].

The aim of the study is to investigate the effects of Myo-inositol on androgen receptor signaling and key cancer-related pathways in castration-resistant prostate cancer (CRPC) through proteomic analysis, with the objective of identifying novel therapeutic targets and developing safer, more effective treatments to improve patient outcomes.

Materials and Methods

Cell culture and determination of IC_{50}

We obtained the prostate adenocarcinoma cell line, DU-145 (ATCC catalog no. CCL-2TM), from the American Type Culture Collection (ATCC) in Manassas, VA, USA. The cells were maintained in Dulbecco's modified Eagle's medium (DMEM) supplemented with 10% fetal bovine serum (FBS), 1% sodium pyruvate, and 1% penicillin-streptomycin, all sources of which were Life Technologies, USA. In a humidified CO_2 incubator at 37°C, the cultures were incubated with a gas mixture of 5% CO_2 and 95% air. Cells were subcultured once they attained 80%–90% confluence, after which the culture medium was refreshed every 72 hours. This investigation utilized cells that had already undergone three to ten passages. Myo-inositol treatment was administered to DU-145 cells at a half-maximal inhibitory concentration (IC_{50}) of 0.6 mg/ml for protein analysis, as outlined in our previous study [9].

Protein preparation and 2-D gel electrophoresis

After trypsinization, DU-145 cells (1×10^5) were treated with Myo-inositol and rinsed three times with cold PBS. After 2 hours at 4°C, cells were lysed in 500 µL of buffer containing 7 M urea, 2 M thiourea, 60 mM DTT, 4% CHPS, 1% PMSF, and 0.4% IPG. The supernatant was collected and kept at -80°C after a 30-minute centrifugation at 16,000 × g. The Bradford assay measured protein concentration. In order to proteome analysis, 50 µg of protein was rehydrated in 300 µL of lysis buffer with 0.001% bromophenol blue and transferred on a 17 cm IPG strip. (pH 4–7). After isoelectric focusing at 80 kVH with a Protein IEF system, a Protein II XL system (Bio-Rad Laboratories, Inc., Philadelphia, PA, USA) performed two-dimensional SDS on a 12% gel. performed at 24 mA per gel. Analysis gels were silver-stained, while preparative gels were Candiano et al.-stained. Methodology Excluded protein regions with significant changes (P-value <0.05 by Student's t-test, >1.5-fold) were measured using PD-Quest software (United States, Philadelphia, PA) [10].

Protein digestion

Cell lysates were produced by acetone precipitation to remove interfering components for protein digestion. The particle received six liters of 80% cold acetone and was incubated overnight at -20°C. Supernatant was discarded. Following a 10-minute centrifugation at 6,000 x g, the particle was dried using a speed vacuum and acetone decanted. The particle was then resuspended in 50 mM ammonium bicarbonate. (8.0 pH). To aid protein digestion, 100 µg protein in 100 µL ammonium bicarbonate was mixed with 0.05% RapigestTM SF, vortexed, and concentrated to 100 µL using a Vivaspin column with a molecular weight cutoff. For 10-15 minutes, heat the mixture at 14,000 rpm (20,800 × g) and then at 80°C for 15 minutes. After reducing with 5 µL of 100 mM DTT for 30 minutes at 37°C, the sample was alkylated with 200 mM iodoacetamide for 45 minutes at room temperature. After overnight incubation at 37°C, 0.2 µg/µL trypsin was added to 5 µL. Add 1 µL of concentrated trifluoroacetic acid (TFA) and heat at 37°C for 20 minutes to stop digestion. After centrifugation, supernatants were kept at −80°C for analysis [11].

LC/MS Analysis

Peptide samples were concentrated to 10 µl each. After mixing with 200 µl of formic acid, the samples were filtered using a 0.45 µm regenerated cellulose membrane syringe filter. Our LC-MS analysis used the Orbitrap Fusion mass spectrometer and Dionex 3000 Ultimate RSLC Nano Liquid Chromatography System (Thermo Fisher Scientific). Analysis using EASY-Spray Column Acclaim PepMapTM C18 (100 Å, 2 µm particle size, 50 µm i.d. × 15 cm) and EASY pre-column. Ion trap mass spectrometry (ITMS) analysed MS2 spectra at a fast scan rate with 60,000 resolving power, 1.0 e2 (100) AGC target, 1.6 m/z separation window, and 250 ms maximum injection length using column C18 (2 cm, 0.1, dm.5 mm) (Figure 1). At 30% and 28% typical collision energies, CID and HCD cleaved the former. Triplicate analyses were done for each sample. Proteome Discover™ software from Thermo Scientific™ was used to examine the raw data [12].

Bioinformatics analysis

Thermo Scientific™ Proteome Discover™ was employed to analyze the peptides that were identified from the unprocessed data. Subsequent analyses implemented three bioinformatics instruments: Panther, Reactom, and Perseus. Panther (Protein Analysis by Evolutionary Correlations) software, version 13.0 (http://pantherb.org/), was employed to further analyze the protein expression profiles generated by Perseus. Panther, which is component of the Gene Ontology Reference Genome Project, offers a comprehensive classification system that includes a curated database of gene, protein, and transcript families, thereby enabling high-throughput analysis. It was implemented to ascertain the molecular activity, protein classification, cellular localization, and biological activity of the identified proteins. Furthermore, Reactome, version 64 (http://reactome.org), a curated pathway database, is employed to offer a comprehensive analysis and interpretation of pathways, thereby enhancing comprehension of the biological processes at play [13].

Statistical analysis

IBM SPSS 26 version was used for statistical analysis. A one-way ANOVA with post-hoc Tukey test was used to draw conclusions from normally distributed data with significant P values ($P<0.05$ and $P<0.001$).

Results

Inhibition of cellular proliferation by Myo-inositol (half maximal inhibitory concentration; IC_{50} in DU-145 cells).

The response to myo-inositol was evaluated using the trypan blue exclusion assay (TBEA) in 6-well plates. DU-145 prostate cancer cells were cultured at a density of 1.0 x 10^5 cells for 72 hours. In MEM media with 10% heat-inactivated FBS, myo-inositol was prepared at a concentration of 50 mg/ml and mixed at concentrations spanning from 0.02 to 0.10 mg/ml (Table 1). After 72 hours of incubation, the IC_{50} of Myo-inositol was 0.06 mg/ml, suggesting a significant inhibitory effect with a dose-dependent decrease in cell viability ($p < 0.05$). Results were displayed as the mean ± SD, and experiments were conducted in triplicate. The statistical significance was evaluated using Tukey's post hoc test and one-way ANOVA.

Cytotoxicity studies of Myo-inositol aqueous solution on mouse skin fibroblast cell line (L929)

We assessed the cytotoxic effects of Myo-inositol on L929 cells after 2 hours of incubation using the IC_{50} dose (0.06 mg/ml). A viability of 89.70% was observed in the morphological evaluation by light microscopy (Figure 2) and cell count, which did not demonstrate any significant difference from untreated cells. According to ISO 10993-5:2009 criteria;less than 20% of cells showing rounding, loose connections, or absence of intracytoplasmic granules;these changes are classified as slight toxicity, indicating no substantial cytotoxic effects from Myo-inositol treatment.

Table 1. Myo-inositol DU145 Cell Numbers and Cell Viability Following Treatment.

Concentration (mg/ ml)	Cell number average (1 x 10^5 cells)	Cell Viability (%)
0	13.20 ± 5.00	100.00 ± 0.00
0.02	10.16 ± 4.04	77.05±2.1
0.04	7.56 ± 5.51	57.32±1.8
0.06	6.63 ± 5.03	50.26±1.2
0.08	5.83 ± 3.06	44.22±0.7
0.1	4.30 ± 7.94	32.46±1.1

** Paired t test

Sequential Extraction Technique after 2-D electrophoresis

Sequential extraction buffers improved protein solubility and separation during 2D-PAGE, allowing for sharper protein spot visibility and possible protein cellular localization (cytoplasmic vs. membrane-associated). Differences in protein spot intensities between control and Myo-inositol-treated groups indicate cellular responses to therapy (Figure 3). 2D gel images of control and treated TRIS extracts showing targeted protein sites for in-gel digestion. Spot numbers match MS analysis and protein database protein lists in Tables 2 and 3. We examined proteins overexpressed in the control group, which were oncogenic, and those in the Myo-inositol-treated group, which were chemopreventive. To study proteins, Uniport numbers, MASCOT scores, molecular weights, isoelectric points, and sequence coverage were cataloged.

Proteins detection

We analyzed Uniport-Mammal and other mass spectrometry data with Thermo ScientificTM Proteome DiscovererTM 2.1. In Chapter 3, a 1% FDR filter produced 415 peptide-spectrum matches (PSMs) with 53 peptide sequences and 192 control sample detections. Myo-inositol-treated samples produced 327 PSMs, 127 peptide sequences, 65 protein groups, 105 proteins, and 23 chemoprevention proteins. Fewer peptides than PSMs were sequenced from these matches due to redundancy and spectral charges. When peptide scores -10lgP, it belongs to one protein category. Protein coverage is the peptide-covered protein sequence. Shared peptide recognition, Uniport entries, species origin, protein summaries, confidence scores, peptide-supported sequence coverage, molecular weights, and high-confidence peptide supports classify proteins in manually prepared (Table 2). Control samples contained cadherin binding, DNA-binding transcription factors, GPCRs, histone acetylation, and extracellular matrix structural proteins. Myo-inositol-treated samples had the greatest DNA-binding

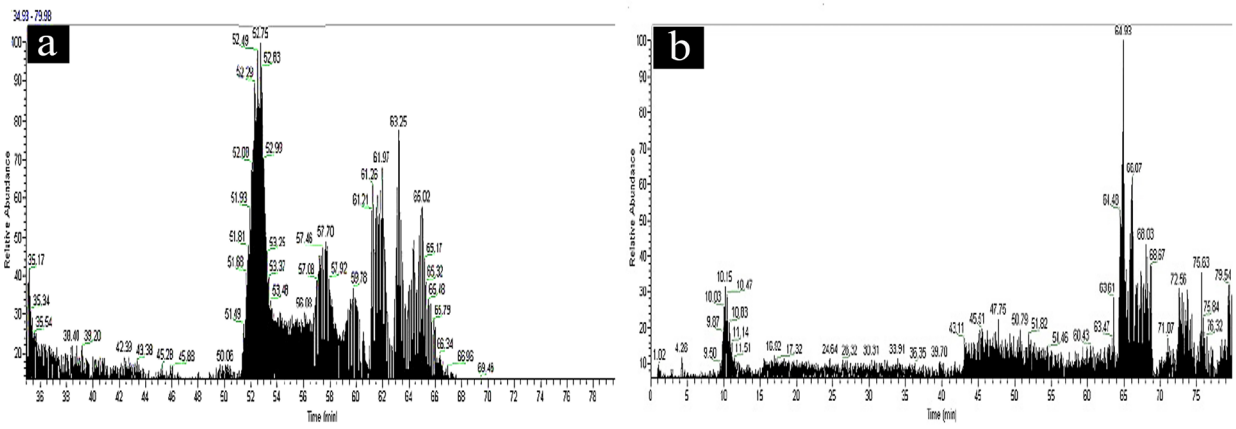

Figure 1. Representation of the Chromatogram Plot and Its associated Spectrum for Control Group (a) and Myo-inositol treated group (b).

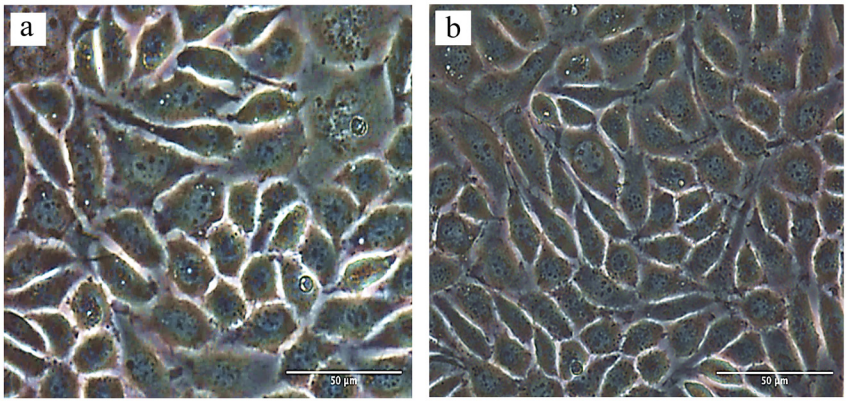

Figure 2. Light Micrographs of L929 Cells with Untreated Control Cells Shown in Image A: following IC_{50} doses of myo-inositol corresponding to Image B: for 72 h incubation. Where images were at 200 x magnification.

transcription factors, followed by DNA repair proteins, Casp8-Associated Protein 2, extracellular matrix structural proteins, and ligand-gated ions (Table 3).

Molecular functions of identified proteins

Panther and Uniport Bioinformatics data analysis tools examined the identified proteins. Figure 4 demonstrates the application of Panther and Uniport protein databases to classify control and myo-inositol treatment samples according to Gene Ontology (GO) annotations for molecular activity. A protein has numerous molecular functions with (GO) designations. Most of the proteins in the control group (48%) ($p < 0.001$) are involved in cytoskeleton protein binding. Cellular stress response activity was followed by 36%. At 9%, transcriptional activity was the least represented molecular activity in the control treatment, while structural molecular activity was at 8%. Most proteins (43.8%) were implicated in the binding process with the myo-inositol therapy group ($P < 0.001$). Transcription regulator activity 4.60%, molecular function regulator activity 4.80%, and molecular transducer activity 5.50%.

Pathways occupied by protein

Bioinformatics tools such as Panther and UniProt were employed to analyze proteins identified in control and Myo-inositol treated groups, with Panther providing classifications based on Gene Ontology (GO) annotations and protein pathways. In the control group, predominant pathways included cytoskeletal regulation via the Wnt signaling pathway (36.7%), cytokine-mediated signaling (25.1%), EGF signaling (14.0%), Rho GTPase

Table 2. List of Identified Proteins in the Control Sample

SL No	Gene name	Protein Description	Accession Number	-10lgP	#Peptides	Sequence coverage (%)
1	*ANXA2*	Annexin A2	P07355	110.05	3	32
2	*TUBB4B*	Tubulin beta-4B chain	P68371	87	4	18
3	*cfl1-a*	Cofilin-1-A	P23528	125.7	2	54
4	*LMNA*	Lamins	P02545	67.75	1	27
5	*FGB*	Fibrinogen beta chain	P02675	81	1	21
6	*PSMB6*	Proteasome subunit beta type 6	P28072	55	1	12
7	*ACTC1*	Actin, alpha 1	P68032	37.33	7	24
8	*PKLR*	Pyruvate kinase	P30613	85.54	13	37
9	*SETD5*	Histone-Lysine N-Methyltransferase	Q9C0A6	11	2	3
10	*TCF20*	Transcription Factor 20	Q9UGU0	5	1	2
11	*GAS2L2*	Gas2-Like Protein 2	Q8NHY3	3	1	2
12	*FUS*	RNA-binding protein FUS	P35637	2	1	2
13	*ZC3H18*	Zinc Finger Cch Domain-Containing Protein 18	Q86VM9	2	1	1
14	*Q15746*	Myosin Light Chain Kinase, Smooth Muscle	MYLK	2	2	2
15	*Q9NYQ7*	Cadherin Egf Lag Seven-Pass G-Type Receptor 3	CELSR3	1	1	1
16	*Q9NRL2*	Bromodomain Adjacent to Zinc Finger Domain Protein 1A	BAZ1A	2	1	1
17	*P02458*	Collagen Alpha-1(II) Chain	COL2A1	3	1	1
28	*Q01955*	Collagen Alpha-3(IV) Chain	COL4A3	2	2	2
19	*Q2LD37*	Transmembrane Protein Kiaa1109	KIAA1109	1	2	1

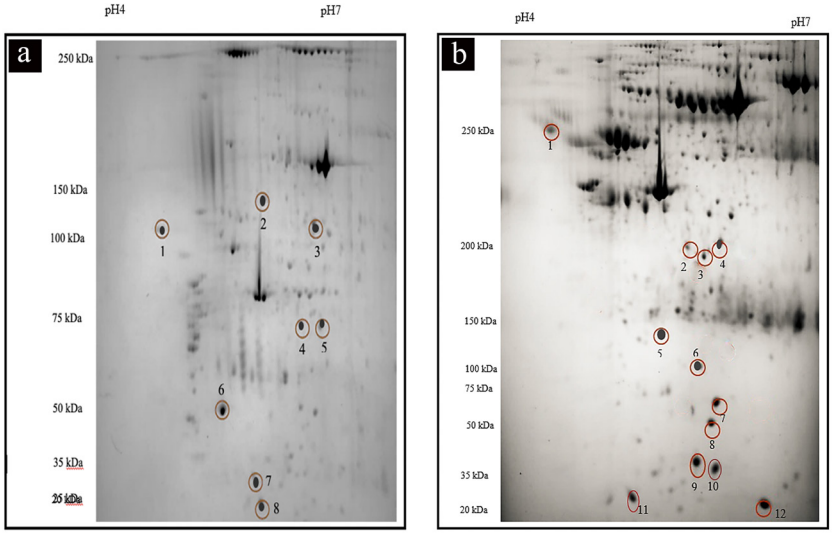

Figure 3. Example of 2-Ddimensional PAGE Analysis of Protein Profile of Control Group (a) and Example of a 2-D dimensional PAGE analysis of protein profile of Myo-inositol treated group (b).

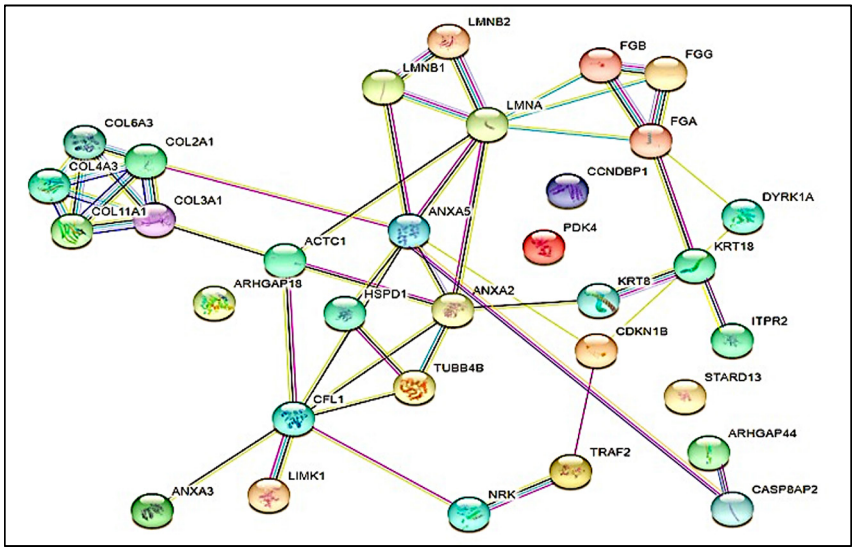

Figure 4. Interaction Networks of Expressed Proteins Identified Using String v 9.11.

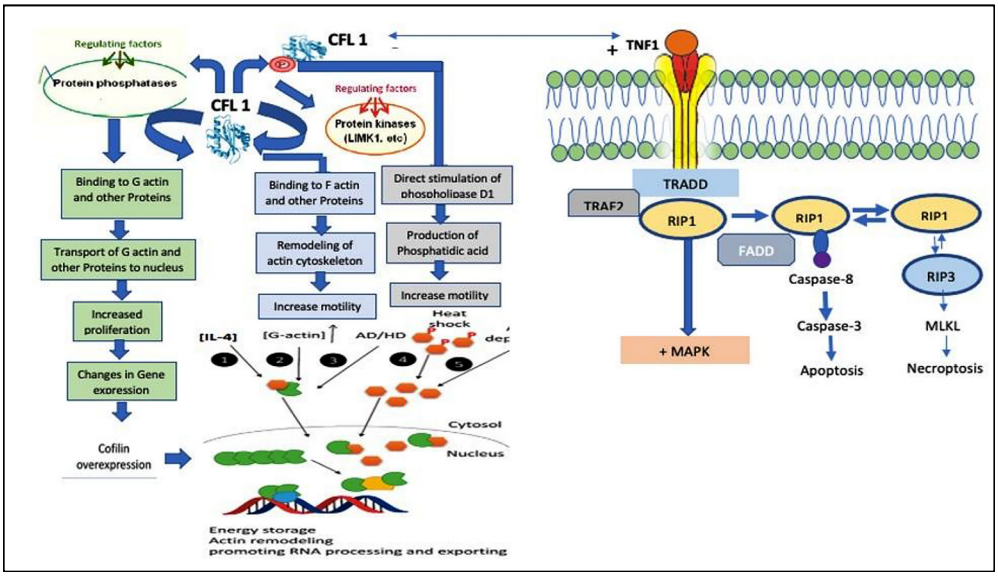

Figure 5. Showing the Schematic Representations of the Mechanism of Myo-Inositol at the Molecular Level on DU-145.

Table 3. List of Proteins in the Myo-Inositol Treatment Sample.

SL No	Gene name	Protein Description	Accession Number	-10lgP	#Peptides	Sequence coverage
1	*ARHGAP1*	Rho GTPase-activating protein	Q07960	65.85	1	37
2	*IFI27*	Haptoglobin (HAP)	P00738	63.1	1	43
3	*APAF1*	Apoptotic protease-activating factor1	O14727	135.14	1	54
4	*TRAF2*	TNF receptor-associated factor 2	Q12933	160.12	1	67
5	*HSPD1*	Heat shock protein 60 kDa	P10809	70.15	3	31
6	*KRT18*	Keratin, type I cytoskeletal 18	P05783	111.09	4	31
7	*KRT8*	Keratin, type II cytoskeletal 8	P05787	60.17	6	27
8	*CCNDBP1*	Cyclin-D1-binding protein 1	O95273	59.87	2	39
9	*CDKN1B*	Cyclin-dependent kinase inhibitor 1B	P46527	68.54	2	32
10	*GSTA1*	Glutathione S transferase P1	P08263	122.38	1	23
11	*ANXA5*	Annexin V	P08758	80.36	2	17
12	*CASP8AP2*	Casp8-Associated Protein	Q9UKL3	9	1	16.5
13	*CAMTA1*	Calmodulin-Binding Transcription Activator 1	Q9Y6Y1	12	2	3
14	*CASP8AP2*	Casp8-Associated Protein 2	Q9UKL3	9	1	16.5
15	*CASP8*	Apoptotic process	Q14790	8	1	3
16	*ITPR2*	Inositol 1,4,5-Trisphosphate Receptor Type 2	Q14571	5	2	3
17	*COL6A3*	Collagen Alpha-3(VI) Chain	P12111	4	1	4
18	*COL3A1*	Collagen Alpha-1(III) Chain	P02461	7	2	4
19	*MXRA5*	Matrix-Remodeling-Associated Protein 5	Q9NR99	9	1	6
20	*KIAA1109*	Transmembrane Protein Kiaa1109	Q2LD37	6	1	6
21	*KRTAP5-10*	Keratin-Associated Protein 5-10	Q6L8G5	6	2	4
22	*PRSS36*	Polyserase-2	Q5K4E3	5	1	4
23	*GABRA4*	Gamma-Aminobutyric Acid Receptor Subunit Alpha-4	P48169	7	1	4

activity (10.4%), and cadherin signaling (14.4%), all essential for cellular functions. For the Myo-inositol treated group, significant pathways involved apoptosis signaling (40.8%, ***p<0.001), p53 pathway feedback (20.8%), heterotrimeric G protein signaling (14.7%), cytokine-mediated inflammation (25.1%), cell cycle regulation (10.4%), and gonadotropin-releasing hormone receptor pathway (11.7%), indicating critical roles in cellular responses to Myo-inositol treatment.

Protein Network Analyses of Protein Interaction Modules

The protein network diagram, illustrating the interrelationships between significant proteins, pathways, and functions, was constructed using STRING version 9.11 (Figure 4). This tool facilitated the identification and connection of key proteins related to the biological activities observed in the study, as depicted in Figure 5. The analysis revealed a densely connected network, where more lines connecting a protein signify greater importance

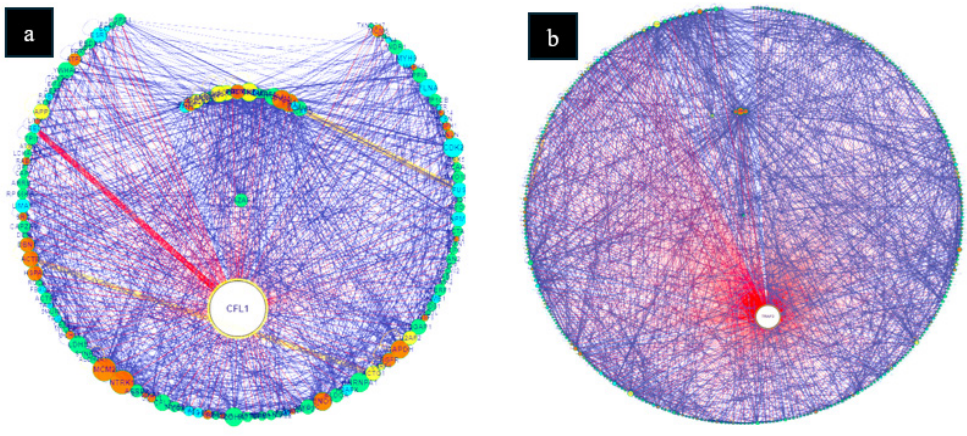

Figure 6. The Interaction Network of CFL1 Proteins was found Using the ChIPP Protein-Protein Interactions Fusion Protein Database. The interaction network of TRAF2 proteins was found utilizing the fusion protein database ChIPP protein-protein interactions.

based on its function. Despite the extensive connectivity, four proteins did not show interactions with core proteins, either due to the absence of Ingenuity Pathway Analysis (IPA) data or a lack of established functional associations. The STRING database, which includes both known and predicted protein-protein interactions, confirms that most proteins specific to this study are interconnected, enhancing the understanding of their collaborative roles in cellular processes.

Chimeric Protein-Protein Interaction (CHIPPI) Analysis

Chimeric Protein-Protein Interaction (ChPPI) is a new technology that classifies conserved chimeric protein interactions using domain-domain co-occurrence scores. Mapping the effects of fusion proteins on cell metabolism and pathways showed that ChPPI networks often induce transcription of oncoproteins and tumor suppressor proteins into the studied proteins. Fusions also provide non-interactor-mediated links between skewed interaction networks and signaling pathways. We found different regulation and myo-inositol-treated community enrichment patterns in the protein PPI network in the prostate cancer cell line DU-145. (Figure 6) depicts CFL-1 and related protein interactions. The fact that CFL-1 is linked to 138 PPIs, 40 of which are onco-proteins, is intriguing.

Discussion

The trypan blue exclusion experiment showed that myo-inositol suppressed the proliferation of the androgen-specific prostate cancer cell line DU-145. The IC_{50} result for Myo-inositol was 0.06 mg/ml over 72 hours, indicating a 50% reduction in DU-145 cell viability. This dose- and time-dependent inhibition suggests Myo-inositol's chemopreventive potential. Myo-inositol's harmful effects were tested on L929 mouse skin fibroblast cell lines, a classic biomaterial cytotoxicity model, before further investigation. According to S. Hussain et al., 2022, this evaluation follows protocols that measure putative anticancer drugs' cytotoxicity in vitro before clinical trials [14]. The IC_{50} dosage of 0.06 mg/ml inhibited less than 11% of L929 cells, making Myo-inositol non-cytotoxic according to ISO standard 10993-5:2009, which requires cell viability above 80%. This profile suggests that Myo-inositol reduces harmful side effects, which is important in developing effective anti-cancer therapies that do not harm healthy cells, supporting M. V. Blagosklonny (2023) and other findings on chemopreventive agent safety [15].

Apaf-1 is a Y-shaped protein with a molecular weight between 133.3 and 141.8 kDa, essential in mitochondrial apoptosis through the formation of the apoptosome upon cytochrome c release, which activates procaspase-9 and subsequent caspases like caspase-3, leading to apoptosis [16]. This study observed a 3-fold increase in Apaf-1 expression, underscoring its importance in apoptosis and as a potential anti-cancer target. TRAF2, part of the TRAF superfamily, regulates NF-kappa-B and JNK pathways essential for cell survival and apoptosis. It interacts with TNFR2 to initiate cell death via Caspase-8. In DU-145 cells, TRAF2 expression increased by 4.4-fold following Myo-inositol treatment, suggesting its role in apoptosis and its potential as a cancer therapeutic target. CKIs regulate cell cycle progression by inhibiting cyclin-dependent kinases (CDKs). The INK4 family targets CDK4/6, while the CIP/KIP family broadly inhibits various cyclin-CDK complexes and can modulate cyclin D-CDK4 complex activity. Following Myo-inositol treatment, CKIs were upregulated 3.3-fold in DU-145 cells, indicating their involvement in cell cycle regulation and potential therapeutic application. CCNDBP1, also known as GCIP, is a 40-kDa protein that suppresses E2F1-mediated transcription, impacting the G1 to S phase transition and serving as a tumor suppressor. It inhibits hepatocellular carcinoma progression and modulates the PI3K/AKT/PTEN pathway. In this study, GCIP expression was upregulated 3-fold, highlighting its role in chemoprevention and its potential as a cancer biomarker and therapeutic target. Annexin V, a 36 kDa protein, binds to phosphatidylserine on apoptotic cell membranes, facilitating their clearance and playing a role in cell differentiation and apoptosis. It also acts as an anticoagulant. This study found a 2.0-fold increase in annexin V expression in prostate cancer cells, pointing to its potential in apoptosis induction and as a therapeutic target in cancer treatment [17-19].

Annexin A2 (ANXA2), with a molecular weight of 40-60 kDa, is implicated in cancer progression by promoting cell division and proliferation, particularly in prostate cancer. It is associated with increased regional lymph node recurrence and metastasis in various cancers, including lymphoma and cervical cancer. ANXA2 influences malignancy through mechanisms like IL-6 secretion and the MAPK pathway and can be downregulated by Myo-inositol in DU-145 prostate cancer cells. Cofilin 1, a ~19 kDa actin-binding protein from the actin-depolymerizing factor (ADF)/cofilin family, plays a vital role in the polymerization and depolymerization of actin filaments, critical for cell motility. Overexpressed in cancer, it facilitates tumor progression through enhanced cell migration, invasion, and metastasis. Cofilin 1 also participates in cytochrome c expression and phospholipase D1 activation under stress conditions. Lamin A/C, approximately 74.13 kDa, is integral to the nuclear lamina, supporting cellular processes such as gene expression, DNA repair, and apoptosis. In prostate cancer, abnormal Lamin A/C expression correlates with tumor grade and proliferation and can be downregulated by Myo-inositol treatment in DU-145 cells. Pyruvate kinase (PK), specifically the *PKM2* isoform, is prevalent in most cancers, including prostate cancer, where it supports metabolic reprogramming from oxidative phosphorylation to glycolysis, facilitating gene replication and cell cycle progression. *PKM2*'s role in cancer cell motility makes it a potential therapeutic target. In DU-145 cells, Myo-inositol treatment resulted in a 4.1-fold decrease in *PKM2* expression [20-22].

Chromosomal translocations in cancer typically lead to the formation of fusion proteins that can disrupt cellular networks by introducing novel protein interactions, driving oncogenesis. The Chimeric Protein-Protein

Interaction (ChiPPI) method [23], which uses a 'domain-domain co-occurrence' (DDCOS) ranking, assesses the likelihood of these interactions and was applied to examine 23 fusion proteins treated with Myo-inositol in this study, mapping changes within both parental and fusion protein networks.

Our analysis revealed that the control group, including Cofilin-1-A, comprised 40 oncoproteins (28.78%), 138 interactors, and 1,286 binary protein-protein interactions (13.41% saturation), highlighting potential fusion events across pathways like Wnt, EGFR, and ATF2 that are crucial for oncogenesis. In contrast, the Myo-inositol-treated group demonstrated enrichment in apoptosis, TGF-β, and p53 pathways, mediated by interactions with TNF receptor-associated factor 2. This group showed 319 interactors, 48 tumor suppressors (15.05%), 1,742 binary PPIs (3.43% saturation), and 53 potential fusions. These findings underscore the role of fusion proteins and network alterations in cancer progression, particularly in influencing pathways targeted by chemopreventive interventions (Figure 6).

In conclusion, finally, Myo-inositol showed notable chemopreventive effects in DU-145 prostate cancer cells, reducing IC_{50} values and enhancing anti-proliferative actions. It prompted apoptosis and cell cycle arrest, evident from cellular and proteomic changes.

Author Contribution Statement

All authors contributed equally in this study.

Acknowledgements

The authors would like to acknowledge department of Pharmacology, Bangabandhu Sheikh Mujib Medical University, Dhaka, Bangladesh.

Approval

The project was approved by the Ethical approval body at the Bangabandhu Sheikh Mujib Medical University, Dhaka, Bangladesh.

Ethical consideration

Ethical issues (including plagiarism, data fabrication, double publication) were completely obliged by the authors.

Conflict of interest

There is no conflict of interest.

References

1. Graham LS, Lin JK, Lage DE, Kessler ER, Parikh RB, Morgans AK. Management of prostate cancer in older adults. Am Soc Clin Oncol Educ Book. 2023;43:e390396. https://doi.org/10.1200/edbk_390396.
2. Rawla P. Epidemiology of prostate cancer. World J Oncol. 2019;10(2):63-89. https://doi.org/10.14740/wjon1191.
3. Narayan V, Ross AE, Parikh RB, Nohria A, Morgans AK. How to treat prostate cancer with androgen deprivation and minimize cardiovascular risk: A therapeutic tightrope. JACC: CardioOncology. 2021;3(5):737-41. https://doi.org/10.1016/j.jaccao.2021.09.014.
4. Kakkat S, Pramanik P, Singh S, Singh AP, Sarkar C, Chakroborty D. Cardiovascular complications in patients with prostate cancer: Potential molecular connections. Int J Mol Sci. 2023;24(8):6984. https://doi.org/10.3390/ijms24086984
5. Hashem S, Ali TA, Akhtar S, Nisar S, Sageena G, Ali S, et al. Targeting cancer signaling pathways by natural products: Exploring promising anti-cancer agents. Biomedicine & Pharmacotherapy. 2022;150:113054. https://doi.org/10.1016/j.biopha.2022.113054.
6. Gonzalez-Uarquin F, Rodehutscord M, Huber K. Myo-inositol: Its metabolism and potential implications for poultry nutrition—a review. Poultry Science. 2020;99(2):893-905. https://doi.org/10.1016/j.psj.2019.10.014.
7. Gonzalez-Uarquin F, Kenéz Á, Rodehutscord M, Huber K. Dietary phytase and myo-inositol supplementation are associated with distinct plasma metabolome profile in broiler chickens. Animal. 2020;14(3):549-59. https://doi.org/10.1017/S1751731119002337.
8. Bizzarri M, Dinicola S, Bevilacqua A, Cucina A. Broad spectrum anticancer activity of myo-inositol and inositol hexakisphosphate. Int J Endocrinol. 2016;2016:5616807. https://doi.org/10.1155/2016/5616807.
9. Islam MJ, Das AK, S M. Cytometry investigation of myo-inositol-induced growth inhibition, apoptosis induction and cell cycle arrest in the human prostate cancer cell line (du-145). Bangladesh J Med Sci. 2024;23(3):655-65. https://doi.org/10.3329/bjms.v23i3.75021.
10. Posch A. Sample preparation guidelines for two-dimensional electrophoresis. Arch Physiol Biochem. 2014;120(5):192-7. https://doi.org/10.3109/13813455.2014.955031.
11. Switzar L, Giera M, Niessen WMA. Protein digestion: An overview of the available techniques and recent developments. J Proteome Res. 2013;12(3):1067-77. https://doi.org/10.1021/pr301201x.
12. Muhammad Nabil1, Azman Seeni1, Wan Ismahanisa Ismail2 and Nurhidayah Ab. Rahim2. Proteomic analysis of anti-cancer effects of streblus asper root extract on hela cancer cells. Biomed Pharmacol J. 2019;12(4):1263-77. https://doi.org/10.13005/bpj/1755.
13. Krüger L, Albrecht CJ, Schammann HK, Stumpf FM, Niedermeier ML, Yuan Y, et al. Chemical proteomic profiling reveals protein interactors of the alarmones diadenosine triphosphate and tetraphosphate. Nat Commun. 2021;12(1):5808. https://doi.org/10.1038/s41467-021-26075-4.
14. Hussain S, Liufang H, Shah SM, Ali F, Khan SA, Shah FA, et al. Cytotoxic effects of extracts and isolated compounds from ifloga spicata (forssk.) sch. Bip against hepg-2 cancer cell line: Supported by admet analysis and molecular docking. Front Pharmacol. 2022;13:986456. https://doi.org/10.3389/fphar.2022.986456.
15. Blagosklonny MV. Selective protection of normal cells from chemotherapy, while killing drug-resistant cancer cells. Oncotarget. 2023;14:193-206. https://doi.org/10.18632/oncotarget.28382.
16. Wu CC, Lee S, Malladi S, Chen MD, Mastrandrea NJ, Zhang Z, et al. The apaf-1 apoptosome induces formation of caspase-9 homo- and heterodimers with distinct activities. Nat Commun. 2016;7:13565. https://doi.org/10.1038/ncomms13565.
17. Siegmund D, Wagner J, Wajant H. Tnf receptor associated factor 2 (traf2) signaling in cancer. Cancers (Basel). 2022;14(16). https://doi.org/10.3390/cancers14164055.
18. Ding L, Cao J, Lin W, Chen H, Xiong X, Ao H, et al. The roles of cyclin-dependent kinases in cell-cycle progression

and therapeutic strategies in human breast cancer. Int J Mol Sci. 2020;21(6). https://doi.org/10.3390/ijms21061960.
19. Li X, Link JM, Stekhova S, Yagle KJ, Smith C, Krohn KA, et al. Site-specific labeling of annexin v with f-18 for apoptosis imaging. Bioconjug Chem. 2008;19(8):1684-8. https://doi.org/10.1021/bc800164d.
20. Wang T, Wang Z, Niu R, Wang L. Crucial role of anxa2 in cancer progression: Highlights on its novel regulatory mechanism. Cancer Biol Med. 2019;16(4):671-87. https://doi.org/10.20892/j.issn.2095-3941.2019.0228.
21. Xu J, Huang Y, Zhao J, Wu L, Qi Q, Liu Y, et al. Cofilin: A promising protein implicated in cancer metastasis and apoptosis. Front Cell Dev Biol. 2021;9:599065. https://doi.org/10.3389/fcell.2021.599065.
22. Dubik N, Mai S. Lamin a/c: Function in normal and tumor cells. Cancers (Basel). 2020;12(12). https://doi.org/10.3390/cancers12123688.
23. Mukherjee SB, Mukherjee S, Frenkel-Morgenstern M. Fusion proteins mediate alternation of protein interaction networks in cancers. Advances in protein chemistry and structural biology. 2022;131:165-76.